Few-Body Syst (2016) 57:255–264
DOI 10.1007/s00601-016-1050-z

H. Kamada · J. Furuya · M. Yamaguchi · S. Oryu

Neutron Pairing Correlations in an α–n–n Three-Cluster Model of the ^{6}He Nucleus

Received: 1 June 2015 / Accepted: 2 February 2016 / Published online: 23 February 2016

Abstract An α–n–n three-cluster model of the ^{6}He nucleus is studied by solving the Faddeev equations, where the cluster potential between α and n takes into account the Pauli exclusion correction, using the Fish-Bone Optical Model (Schmid in Z Phys A 297:105, 1980). The resulting binding energy of the ground state (0^+) is 0.831 MeV and the resonance energy of the first excited state (2^+), 0.60−i0.012 MeV, is extracted from the three-cluster break-up threshold. These theoretical values are in reasonable agreement with the experimental data: 0.973 MeV and 0.824−i0.056 MeV, respectively. In order to investigate the structure of these states, we calculate the angle density matrix for the $\angle n_1\alpha n_2$ angle in the triangle formed by the three clusters. The angle density matrix of the ground state has two peaks and the configuration of 0^+ wave function corresponding to the peaks constitutes a mixture of an acute-angled triangle structure and an obtuse-angled one. This finding is consistent with the former result from a variational approach (Hagino and Sagawa in Phys Rev C 72:044321, 2005). On the other hand, in the case of 2^+ state only a single peak is obtained.

1 Introduction

Recently, neutron rich nuclei have been vigorously measured at RIKEN and GSI. The ^{6}He nucleus plays a special role in these investigations, because its neutron halo skin structure can be easily attributed to the picture that it consists of the α core and weakly correlated two neutrons. This three-cluster system was investigated within the Faddeev framework by Eskandarian and Afnan [3], however, their investigation was restricted to the isospin $T = 1$ in ^{6}Li and neglected the Coulomb force.

In this paper we employ the Fish-Bone Optical Model (FBOM) [1] to the α–n potential. Using the Orthogonality Condition Model (OCM) [4], one aims to remove Pauli forbidden states (PFS) from the cluster wave function. Still, despite the fact that OCM is applied [5] to the three-alpha cluster model of ^{12}C nucleus, some spurious states corresponding to the PFS were observed. On the other hand, not only the PFS but also the almost PFS (APFS) are correctly treated in the FBOM [1]. It was shown in [6] that the three-cluster calculation with the FBOM potential does not lead to such spurious states at all. The potential was expanded in a separable

H. Kamada (✉) · J. Furuya
Department of Physics, Faculty of Engineering, Kyushu Institute of Technology, 1-1 Sensuicho Tobata, Kitakyushu 804-8550, Japan
E-mail: kamada@mns.kyutech.ac.jp

M. Yamaguchi
Research Center for Nuclear Physics, Osaka University, 10-1 Mihogaoka, Ibaraki, Osaka 567-0047, Japan
E-mail: yamagu@rcnp.osaka-u.ac.jp

S. Oryu
Department of Physics, Tokyo University of Science, Noda, Chiba 278-8510, Japan
E-mail: oryu@rs.noda.tus.ac.jp

form by Unitary Interpolation Method [7]. A new parametrization of the FBOM of the α–n potential appeared recently [8], however, we employ here the original version [7]. We follow the calculation of the former work [3] and obtain the wave function from the FBOM potential.

In following Sects. 2 and 3 we will explain the cluster potentials of α–n and n–n, and the Faddeev three-body equations. Results for the binding energies, the components of the wave function and the expectation values of the potential for the ground state 0^+, are discussed in Sect. 4. We use an additional scheme (Complex Energy Method [9]) for the resonance state 2^+.

In Sect. 5, in order to investigate the inner structure of the wave function, we calculate an angle density matrix which was introduced by Hagino and Sagawa [2]. They used various Hamiltonians which were made with a density-dependent contact interaction by fitting the corresponding differential cross section of the subsystem [10]. However, their variational calculation displayed spurious states (deeply bound s states) [10] below their ground states. Thus we study wave functions obtained from different Hamiltonians and compare our predictions with the angle density matrices given in literature. Summary will be given in Sect. 6.

2 The α–n Interaction

The potentials in our study have a separable form. The Unitary Interpolation Method [7] is applied to the Fish-Bone Optical Model of the α–n interaction [1]. This potential is restricted to low partial waves: $l_j = \mathrm{S}_{1/2}$, $\mathrm{P}_{3/2}$ and $\mathrm{P}_{1/2}$, where l and j denote the angular momentum and the total angular momentum, respectively. The potential $V^{sep}(p, p')$ has a following form;

$$V^{sep}_{l_j}(p, p') = \sum_{m,n} g_{l_j,m}(p) \Lambda^{l_j}_{m,n} g_{l_j,n}(p') \tag{1}$$

with the form factor $g_{l_j,m}(p)$:

$$g_{l_j,m}(p) = \sum_{\nu} \alpha^{l_j}_{\nu,m} u^{l_j}_{\nu}(p), \tag{2}$$

where $\Lambda^{l_j}_{m,n}$ and $\alpha^{l_j}_{\nu,m}$ are the coupling constants and the coefficients of the expansion into the harmonic oscillator functions $u^{l_j}_{\nu}(p)$ with the principal quantum number ν, respectively. The separable form satisfies the modified Lippmann-Schwinger equation:

$$\tau^{l_j}_{mn}(E_2) = \Lambda^{l_j}_{mn} + \sum_{s,t} \Lambda^{l_j}_{ms} \int_0^{\infty} \frac{g_{l_j,s}(p) g_{l_j,t}(p)}{E_2 - p^2/2\mu} p^2 dp \; \tau^{l_j}_{tn}(E_2), \tag{3}$$

where E_2 is the center of mass energy of the α–n two-body system. The propagator $\tau^{l_j}_{mn}$ is substituted into the Faddeev equation (Eq. (9)) in the next section. The ranks of the matrices Λ and τ are 3, 2 and 2 for $\mathrm{S}_{1/2}$, $\mathrm{P}_{3/2}$ and $\mathrm{P}_{1/2}$, respectively.

The FBOM potential treats correctly the Pauli exclusion principle among the two clusters [1]. In particular, the coupling constant Λ in Eq. (1) with respect to the PFS is prepared to produce a huge repulsion ($\Lambda^{\mathrm{S}_{1/2}}_{11} = 99981.8816\,\mathrm{MeV}$)[7]. In Figs. 1, 2, and 3 we demonstrate the form factors $g_{l_j,n}(p)$ for each partial wave. For instance, the form factor $g_{S_{1/2},1}(p)$ corresponds to a PFS [7].

For the sake of the comparison with the former study [3] we keep the same n–n potential, with Eskandarian and Afnan's form factor given as a simple rank 1 Yamaguchi type:

$$g_{l_j,1}(p) = \frac{p^l}{\left(p^2 + \beta^2_{l_j}\right)^{l+1}}. \tag{4}$$

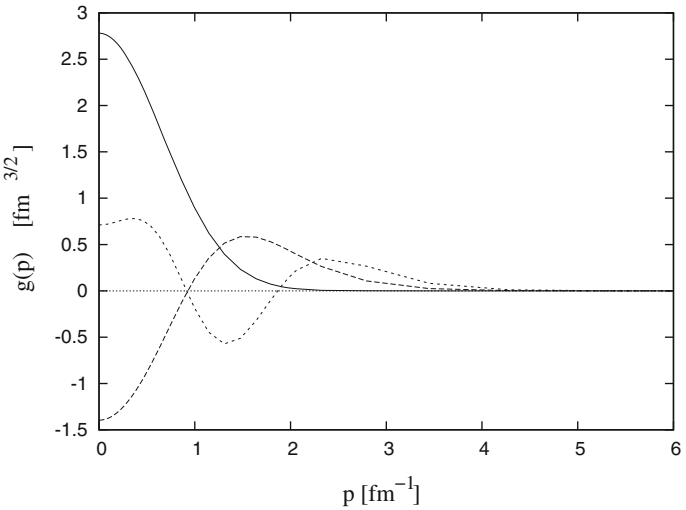

Fig. 1 Form factors $g_{l_j,m}(p)$ for $S_{1/2}$ of the α–n potential. The *solid*, *dashed* and *short-dashed* lines are for rank $m = 1, 2$ and 3, respectively

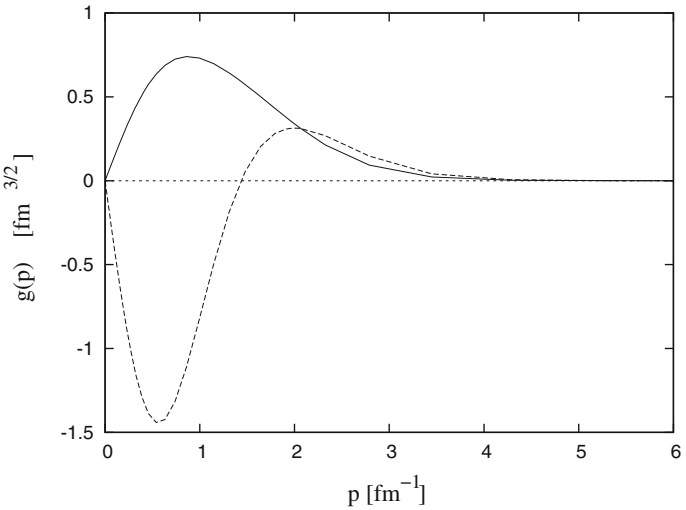

Fig. 2 Form factors $g_{l_j,m}(p)$ for $P_{3/2}$ of the α–n potential. The *solid* and *dashed lines* are for rank $m = 1$ and 2, respectively

3 Three-Body Formalism

The separable method of the three-body Faddeev formalism was introduced in the textbook of Afnan and Thomas [11] in detail. Also the representation of the α–n–n system follows the formalism which was prepared for the similar case of α–α–Λ system [12]. Therefore, we refer the reader to [12] for details and restrict ourselves to a very brief description of our formalism.

We denote the set of z-components for the three particles' spins $(\sigma_1, \sigma_2, \sigma_3)$ by $\mathbf{d} = (d_1, d_2, d_3)$. Then the free three-body state in Faddeev particle channel i is given by $|\mathbf{p}_i \mathbf{q}_i \mathbf{d}_i\rangle$, where $\mathbf{p}_i$ and $\mathbf{q}_i$ are the two (relative) Jacobi momentum vectors, respectively. This state vector is represented by usual couplings of the orbital angular momenta and spins. We introduce a standard spin-angular-momentum coupling scheme $\sigma_j + \sigma_k = s_i$, $s_i + l_i = j_i$, $j_i + \sigma_i = K_i$, and $K_i + L_i = J$, where J is the total angular momentum of the system with the corresponding z-component M. Here we can define a state channel N_i corresponding to the particle channel i:

$$N_i \equiv [\{((l_i s_i) j_i \sigma_i) K_i L_i\}]. \tag{5}$$

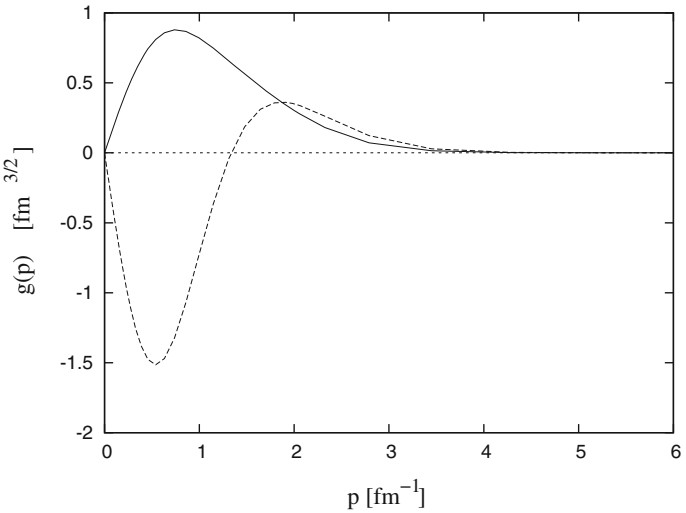

Fig. 3 Form factors $g_{l_j,m}(p)$ for $P_{1/2}$ of the α–n potential. The lines are the same as in Fig. 2

Therefore, we have

$$\begin{aligned}|\mathbf{p}_i\mathbf{q}_i\mathbf{d}\rangle &= \sum_{l_i s_i j_i K_i L_i J} |p_i q_i (l_i s_i) j_i K_i L_i J\rangle \sum_{M_{l_i} M_{s_i} M_{j_i} M_{K_i} M_{L_i} M} \\ &\times \langle \sigma_j d_j \sigma_k d_k | s_i M_{s_i}\rangle \langle l_j M_{l_j} s_i M_{s_i} | j_i M j_i\rangle \langle j_i M_{j_i} \sigma_i d_i | K_i M_{K_i}\rangle \\ &\times \langle K_i M_{K_i} L_i M_{L_i} | J M\rangle Y_{l_i M_{l_i}}(\hat{\mathbf{p}}_i) Y_{L_i M_{L_i}}(\hat{\mathbf{q}}_i) \\ &= \sum_{N_i} |p_i q_i N_i\rangle\langle N_i | \hat{\mathbf{p}}_i \hat{\mathbf{q}}_i \mathbf{d}\rangle. \end{aligned} \tag{6}$$

The wave function Ψ^{J^π} consists of three Faddeev components $\psi_i^{J^\pi}$, ($i = 1, 2$ and 3),

$$\Psi^{J^\pi} = \psi_1^{J^\pi} + \psi_2^{J^\pi} + \psi_3^{J^\pi}, \tag{7}$$

while the Faddeev component is represented in the partial-wave basis:

$$\begin{aligned}\psi_i^{J^\pi}(\mathbf{p}_i, \mathbf{q}_i) &= \left\langle \mathbf{p}_i\mathbf{q}_i\mathbf{d} | \psi_i^{J^\pi}\right\rangle \\ &= \sum_{N_i}\sum_{m,n} \frac{1}{E - p_i^2/2\mu_i - q_i^2/2\nu_i} g_m^{l_i(N_i)}(p_i)\tau_{m,n}^{l_i(N_i)}(E - q_i^2/2\nu_i) f_{N_i,n}^{J^\pi}(q_i)\langle N_i|\hat{\mathbf{p}}_i\hat{\mathbf{q}}_i\mathbf{d}\rangle, \end{aligned} \tag{8}$$

where $f_{N_i,n}^{J^\pi}$ is called the reduced wave function and it satisfies the Amado–Lovelace–Mitra equations;

$$\begin{aligned} f_{N_i,n}^{J^\pi}(q_i) = \sum_{k=1}^{3}\sum_{N_k,m,t}\int_0^\infty & Z_{N_i,N_k,n,m}^{J^\pi}(q_i, q_k; E)\tau_{m,t}^{l_k(N_k)}(E - q_k^2/2\nu_k) \\ &\times f_{N_k,t}^{J^\pi}(q_k) q_k^2 dq_k/2\pi^2. \end{aligned} \tag{9}$$

Here μ_i and ν_i denote the reduced masses of two-body and three-body system [12]. In practical numerical calculations we introduce discretization grids with integral points so the integral kernel becomes a matrix and Eq. (9) is turned into an eigenvalue problem:

$$[Z(E)][\tau]\mathbf{f} = \eta\,\mathbf{f}, \tag{10}$$

where the eigenvalue η is required to be 1, when the three-body energy E coincides with the binding energy $E = E_b$. The integral kernel $Z(E)$ in Eq. (9) is given as

$$Z^{J^\pi}_{N_i N_j}(q_i, q_j; E) = (1-\delta_{ij}) q_i^{l_i} q_j^{l_j} \sum_{\mathcal{L}=0}^{(l_i+l_j+L_i+L_j)/2} F^{\mathcal{L}}_{N_i N_j}(q_i, q_j) \sum_{a,b} A^{\mathcal{L}ab}_{N_i N_j} (q_j/q_i)^{b-a} \tag{11}$$

with

$$F^{\mathcal{L}}_{N_i N_j}(q_i, q_j; E) = \frac{1}{2} \int_{-1}^{1} \frac{g_{N_i}(p_i) g_{N_j}(p_j) p_i^{-l_i} p_j^{-l_j} P_{\mathcal{L}}(\cos\theta)}{E - q_i^2/2m_i - q_j^2/2m_j - (\mathbf{q}_i + \mathbf{q}_j)^2/2m_k} d\cos\theta, \tag{12}$$

where $P_{\mathcal{L}}$ is the Legendre polynomial and the coefficient $A^{\mathcal{L}ab}_{N_i N_j}$ in Eq. (9) is the recoupling coefficient introduced in the textbook of Afnan and Thomas [11]. Note that in our former paper [12] important information about the phase of the recoupling coefficients is provided.

Later we need the modified wave function $F^{J^\pi}_{N_i m}(q_i)$ which is defined as

$$F^{J^\pi}_{N_i m}(q_i) \equiv \sum_n \tau^{l_i(N_i)}_{mn}(E - q_i^2/2\nu_i) f^{J^\pi}_{N_i n}(q_i). \tag{13}$$

4 Calculation and Results

Partial wave approximation for the 2-cluster potential is taken into account only up to p-wave in the α–n subsystem and $^1S_0$ in n–n one. The ground bound state 0^+ of the ^{6}He nucleus consists of seven state channels, as shown in Table 1. The particle channels (subsystem clusters)spectator=$(\alpha n_2)n_1$, $(n_1\alpha)n_2$ and $(n_1 n_2)\alpha$ are labelled 1, 2 and 3, respectively. The numerical integrals are carried out using the Gauss–Legendre method and the same grid points are employed to solve the Faddeev equation (10) by the Gauss–Seidel method, where the size of the discretized matrix is about $(3 \times 7 \times \text{rank} \times \text{number of integral points})^2$. Table 2 shows the binding energies of our model and the ones obtained in the former study [3]. For the sake of comparison, the other binding energies calculated with several different schemes and potentials are demonstrated in Table 2. The calculations of Refs. [13,14] take explicitly the PFS between α–n into account but in the form of the APFS.

Although the FBOM binding energy of the ground state is closer to the experimental value than the other predictions, it can be hardly argued that the Hamiltonian reached a high degree of accuracy; there is definitely room for improvement. From ab initio Green's Function Monte Carlo calculations [17] it is known that a contribution from the three-nucleon force is required (ΔE_α= 4.30 MeV) in order to construct a properly bound

Table 1 The channels for the ground state $J^\pi = 0^+$

Angular momentum\particle channel	1,2	1,2	1,2	3
L	0	1	1	0
K	0	1	1	0
j	1/2	3/2	1/2	0
l	0	1	1	0
s	1/2	1/2	1/2	0
Label of the state channel	$S_{1/2}$	$P_{3/2}$	$P_{1/2}$	$^1S_0$

Table 2 The calculated binding energies E_b and the resonance ones E_1 compared with the other model calculation and the experimental data in MeV

	Model and Scheme	E_b (0^+)	E_1 (2^+) = $E_{(\text{real part})} - i\Gamma/2$
Kukulin et al. [13]	Variational	−0.138	1.463
Zhukov et al. [14]	Hyperspherical Harmonics, Faddeev	−0.4	
Suzuki [15]	Cluster-orbital shell model	−0.50	
Eskandarian et al. [3]	Model A, Faddeev calculation	−0.56	0.95−i 0.15
Present works	Pauli Corrected, Faddeev calculation	−0.831	0.60−i 0.012
Exp. [16]	–	−0.973	0.824−i 0.056

Table 3 Components of the state $J^\pi = 0^+$

Particle channel	State channel	Direct (%)	Exchange (%)	Total (%)
1,2	$S_{1/2}$	1.5	−1.8	−0.3
1,2	$P_{3/2}$	18.1	17.2	35.3
1,2	$P_{1/2}$	0.5	1.0	1.5
3	$^1S_0$	21.3	5.7	27.0
Total	–	61.5	38.5	100

Table 4 Expectation values of the potential for SC in $J^\pi = 0^+$

Particle channel	State channel	Direct (MeV)	Exchange (MeV)	Total (MeV)
1,2	$S_{1/2}$	−0.4	−0.1	−0.5
1,2	$P_{3/2}$	−6.2	−4.8	−11.0
1,2	$P_{1/2}$	−0.1	−0.3	−0.4
3	$^1S_0$	−3.1	−2.4	−5.5
Total	–	−16.5	−12.8	−29.3

α particle. [1] Similarly, the contribution of the three-nucleon force is necessary ($\Delta E_{^6\mathrm{He}}$=5.48 MeV) to build the ^{6}He nucleus with the proper binding energy. A rough estimate of the contribution of the three-cluster force in the α–n–n system can be the difference $\Delta E_{^6\mathrm{He}} - \Delta E_\alpha$ = 1.18 MeV. However, the core nucleus α inside ^{6}He might be very dense and the contribution of the three-nucleon force in the core could become larger. Our cluster model does not treat such a core excitation.

Recently, we introduced a cluster model [18], which explicitly incorporated the core excitation for the neutron rich nuclei ^{8}He and ^{10}He. In the case of ^{8}He (^{10}He) the core nucleus ^{6}He (^{10}He) has an excited state 2^+ whose energy spectrum is close to the ground state one. In our present model the energy of the excitation state of the core nucleus α is very far from the ground state one. Consequently, in the α–n–n system we could see that the difference ($\Delta E_{^6\mathrm{He}} - \Delta E_\alpha$) of the three-cluster force originates mainly from the three-nucleon force inside the core nucleus α.

The total wave function Ψ is normalized by

$$1 = \left\langle \Psi^{J^\pi} | \Psi^{J^\pi} \right\rangle = \sum_{i=1}^{3} \left\langle \psi_i^{J^\pi} | \psi_i^{J^\pi} \right\rangle + \sum_{i \neq j}^{6} \left\langle \psi_i^{J^\pi} | \psi_j^{J^\pi} \right\rangle, \tag{14}$$

where the first sum on the right-hand side is called the direct component and the second one comprises the exchange components. These quantities are shown in Table 3 for the few considered state channels. We thus observe that the wave function consists mainly of the $P_{3/2}$ state channel (70.6 %=35.3 %×2) and the $S_{1/2}$ state channel is suppressed because of FBS and AFBS.

In addition to the wave function components, Table 4 shows the expectation values of the potential for the state channel. These expectation values are defined as

$$\left\langle \Psi^{J^\pi} | V | \Psi^{J^\pi} \right\rangle = \sum_{i=1}^{3} \left\langle \psi_i^{J^\pi} | G_0^{-1} | \psi_i^{J^\pi} \right\rangle + \sum_{i \neq j}^{6} \left\langle \psi_i^{J^\pi} | G_0^{-1} | \psi_j^{J^\pi} \right\rangle, \tag{15}$$

where the first sum on the right-hand side gives the so-called direct expectation values and the second term yields the exchange expectation values. These potential expectation values reveal a similar tendency to the components of the wave function. It is clear that the largest contribution comes from the $P_{3/2}$ partial wave.

Next we concentrate on the first excited state 2^+. In this case we have 17 state channels as shown in Table 5. The integral kernel of the three-body Green's function (G_0) generates a singularity in the continuum state region ($E > 0$) and a suitable method has to be used to deal with this type of the Faddeev equation. Our choice is the Complex Energy Method (CEM) [9], recently successfully applied to several nuclear systems [19–21]. Using the CEM we obtain a FBOM resonance state 2^+ and the result is shown in Table 2.

[1] In [17] the realistic Argonne V18 nucleon–nucleon potential and the Illinois-2 version of the three-nucleon force was used.

Table 5 The state channels for the excited state $J^{\pi} = 2^{+}$

Angular momentum\particle channel	1,2	1,2	1,2	1,2	1,2	1,2	1,2	1,2	3
L	2	2	1	3	1	3	1	3	2
K	0	1	1	1	1	1	2	2	0
j	1/2	1/2	1/2	1/2	3/2	3/2	3/2	3/2	0
l	0	0	1	1	1	1	1	1	0
s	1/2	1/2	1/2	1/2	1/2	1/2	1/2	1/2	0

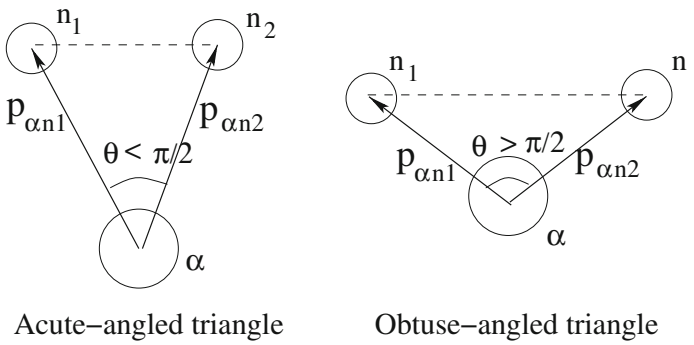

Fig. 4 The acute-angled triangle and obtuse-angled triangle three-cluster α–n–n configurations in the ^{6}He nucleus

5 The Angle Density Matrix

In order to investigate the inner structure of the wave function we calculate the angle density matrix $\rho(\theta)$, which was introduced by Hagino Sagawa [2]:

$$\rho(\theta) = \frac{1}{2\pi}\langle\Psi|\delta(\tilde{\theta} - \theta)|\Psi\rangle \tag{16}$$

with

$$\cos\tilde{\theta} = -\frac{\mathbf{p}_{\alpha n_1} \cdot \mathbf{p}_{\alpha n_2}}{|\mathbf{p}_{\alpha n_1}|\,|\mathbf{p}_{\alpha n_2}|}, \tag{17}$$

where the vectors $\mathbf{p}_{\alpha n_1}$ and $\mathbf{p}_{\alpha n_2}$ are the relative momenta between the α–n. There are two typical configurations of the three-body system in question. In the first case an acute-angled triangle (di-neutron) is formed and in the second one an obtuse-angled triangle (cigar-like) shape arises. Figure 4 illustrates the definition of the angle $\theta = \angle n_1 \alpha n_2$.

Figure 5 shows the angle density matrix $\rho(\theta)$, which is normalized as

$$2\pi \int_0^{\pi} \rho(\theta) \sin\theta d\theta = 1. \tag{18}$$

The solid (long-dashed) line in this figure shows the angle density matrix of the 0^{+} state obtained with the FBOM and using the potential from [3]. The percentage contributions from the acute-angled and obtuse-angled triangle configurations are integrated from $\theta = 0$ to $\pi/2$. The resulting integrated contributions for each configuration are shown in Table 6. In the case of FBOM potential the two configurations appear nearly equally often in the three-body system. In the calculation with the potential from [3], the acute-angled triangle configuration clearly dominates. Looking at Fig. 4 of [2] one can see that the corresponding result from that work lies between our two predictions. It is very interesting to see that our result is consistent with the prediction obtained using the variational approach, which is derived from a phenomenological single-particle Hamiltonian [10].

We try to visualize the angle density matrix of the resonance state. Since the resonance state belongs to the continuum, the norm of its wave function is not well defined. We thus replace the original wave functions with approximate ones, which correspond to the eigenvalue $\eta = 0.96$ at $E = 0.0$ MeV. Figure 5 shows the short-dashed (dotted) line of the angle density of the state 2^{+} obtained with the FBOM (Eskandarian–Afnan [3]) potential. In both cases a single broad peak at $\theta \approx 60^{\circ}$ is visible.

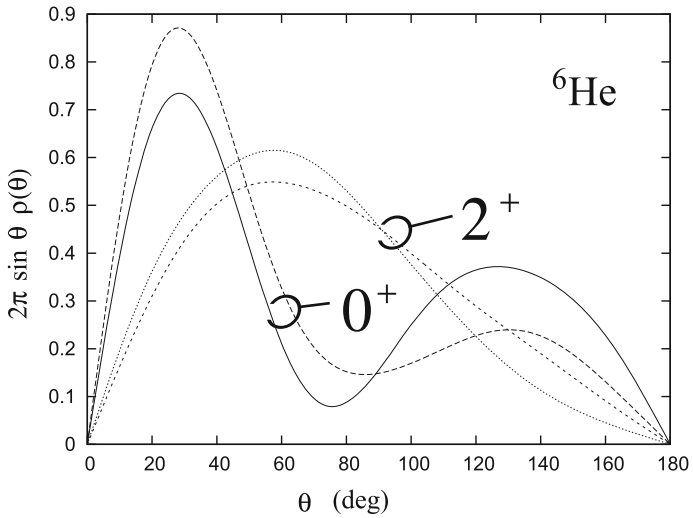

Fig. 5 The angle density matrix $\rho(\theta)$. The *solid* and *long-dashed* (*short-dashed* and *dotted*) lines are calculated from FBOM[7] and Eskandarian–Afnan [3] potentials for the ground state 0^+ (the excited state 2^+), respectively

Table 6 Percentage contributions of the acute-angled triangle and obtuse-angled triangle configurations in the ground state

Potential\configuration	Acute-angled triangle (%)	Obtuse-angled triangle (%)
FBOM [7]	57.8	42.2
Eskandarian–Afnan [3]	72.3	27.7

6 Summary

We solved the Faddeev equation of the α–n–n model to obtain the ground state 0^+ and the first excited state 2^+ of the ^{6}He nucleus. Using the Fish-Bone Optical Model [1] for α–n potential we get the binding energy -0.831 MeV and the resonance energy of $0.60-$i 0.012 MeV. These values compare rather well with the experimental data: -0.973 MeV and $0.824-$i 0.056 MeV, respectively. The partial wave $P_{3/2}$ is the most important component of the ground bound state, since its contribution amounts to 70.6 %. We calculated the angle density matrices, which were introduced by Hagino and Sagawa [2], to study the structure of these wave functions. The angle density matrix of 0^+ has two peaks whose configurations are illustrated as an acute-angled triangle and an obtuse-angled one. Our percentage contribution of the obtuse-angled triangle part is larger than the one obtained from Eskandarian–Afnan because the Pauli exclusion correction is taken into account in our α–n cluster potential. In addition, our angle density matrix and the one shown in [2] reveal a considerable similarity. Contrary to the ground state, the angle density of the resonance state gives only a single peak.

As the natural extension of the present work, we plan to investigate the angle density matrices of other neutron-rich nuclei.

Acknowledgments One of authors (H.K.) would like to thank H. Witała, J. Golak and R. Skibiński for fruitful discussions during his stay at the Jagiellonian University in Kraków. The numerical calculations were partially performed on the interactive server at RCNP, Osaka University, Japan, and on the supercomputer cluster of the JSC, Jülich, Germany.

Appendix

The angle density matrix was introduced in Sect. 5. It reads

$$\rho(\theta) = \frac{1}{2\pi}\langle\Psi|\delta(\tilde{\theta}-\theta)|\Psi\rangle = \frac{1}{2\pi\,\sin\theta}\sum_{\tilde{l}}\frac{(2\tilde{l}+1)}{2}P_{\tilde{l}}(\cos\theta)\langle\Psi|P_{\tilde{l}}(\cos\tilde{\theta})|\Psi\rangle, \tag{19}$$

where the cosine of the angle $\tilde{\theta}$ is written as

$$\begin{aligned}\cos\tilde{\theta} &= -\frac{\mathbf{p}_{\alpha n_1}\cdot\mathbf{p}_{\alpha n_2}}{\left|\mathbf{p}_{\alpha n_1}\right|\left|\mathbf{p}_{\alpha n_2}\right|} \\ &= \frac{\zeta q_i^2+\zeta q_j^2+(1+\zeta^2)q_iq_jx}{\sqrt{q_j^2+\zeta^2q_i^2+2q_iq_j\zeta x}\sqrt{q_i^2+\zeta^2q_j^2+2q_iq_j\zeta x}}\end{aligned} \tag{20}$$

with $x=\cos\theta_{\mathbf{q}_i\mathbf{q}_j}=\frac{\mathbf{q}_i\cdot\mathbf{q}_j}{|\mathbf{q}_i||\mathbf{q}_j|}$ and $\zeta=\frac{m_n}{m_n+m_\alpha}$.

On the other hand, the wave function is approximately represented by using the orthonormality of the UIM form factor [7]

$$\Psi^{J^\pi}_{N_i}(p_i,q_i)=\sum_n g_{N_i,n}(p_i)\left\{G_0F^{J^\pi}_{N_i,n}(q_i)+f^{J^\pi}_{N_i,n}(q_i)\right\}, \tag{21}$$

where $f^{J^\pi}_{N_i,n}(q_i)$ and $F^{J^\pi}_{N_i,n}(q_i)$ are defined in Eqs. (8) and (13), respectively. We use both wave functions $\Psi^{J^\pi}_{N_1}$ and $\Psi^{J^\pi}_{N_2}$ to calculate the expectation values of the Legendre polynomial with the argument $\cos\tilde{\theta}$

$$\begin{aligned}\langle\Psi_1|P_{\tilde{l}}(\cos\tilde{\theta})|\Psi_2\rangle &= \int_0^\infty q_1^2dq_1\int_0^\infty q_2^2dq_2\sum_{N_1,N_2,n,k} \\ &\{F^{J^\pi}_{N_1,n}(q_1)Z^{\tilde{l}(2)}_{N_1,N_2,n,k}(q_1,q_2)F^{J^\pi}_{N_2,k}(q_2)+F^{J^\pi}_{N_1,n}(q_1)Z^{\tilde{l}(1)}_{N_1,N_2,n,k}(q_1,q_2)f^{J^\pi}_{N_2,k}(q_2) \\ &+f^{J^\pi}_{N_1,n}(q_1)Z^{\tilde{l}(1)}_{N_1,N_2,n,k}(q_1,q_2)F^{J^\pi}_{N_2,k}(q_2)+f^{J^\pi}_{N_1,n}(q_1)Z^{\tilde{l}(0)}_{N_1,N_2,n,k}(q_1,q_2)f^{J^\pi}_{N_2,k}(q_2)\}\end{aligned} \tag{22}$$

with

$$\begin{aligned}Z^{\tilde{l}(y)}_{N_i,N_j,n,k}(q_i,q_j) &\equiv {}_i\langle g_nG_0^yP_{\tilde{l}}(\cos\tilde{\theta})g_k\rangle_j \\ &= (1-\delta_{ij})q_i^{l_i}q_j^{l_j}\sum_{\mathcal{L}}^{\mathcal{L}_{max}}F^{\mathcal{L}\tilde{l}(y)}_{N_i,N_j}(q_i,q_j;E)\sum_{a=0}^{l_i}\sum_{b=0}^{l_j}A^{\mathcal{L}ab}_{N_i,N_j}(q_j/q_i)^{b-a}\end{aligned} \tag{23}$$

and

$$F^{\mathcal{L}\tilde{l}(y)}_{N_i,N_j}(q_i,q_j;E)=\frac{1}{2}\int_{-1}^{1}\frac{g_{N_i}(p_i)g_{N_j}(p_j)p_i^{-l_i}p_j^{-l_j}P_{\mathcal{L}}(x)P_{\tilde{l}}(\cos\tilde{\theta})}{(E-q_j^2/2m_i-q_j^2/2m_j-(\mathbf{q}_i+\mathbf{q}_j)^2/2m_k)^y}dx. \tag{24}$$

The maximal value of $\tilde{l}$ is 5, which is sufficient to obtain converged results.

References

1. Schmid, E.W.: The two-cluster "Fish-Bone" model. Z. Phys. A **297**, 105 (1980)
2. Hagino, K., Sagawa, H.: Pairing correlations in nuclei on the neutron-drip line. Phys. Rev. C **72**, 044321 (2005)
3. Eskandarian, A., Afnan, I.R.: $\alpha-d$ resonances and the low-lying states of ^{6} Li. Phys. Rev. **46**, 2344 (1992)
4. Saito, S.: Effect of Pauli principle in scattering of two clusters. Prog. Theor. Phys. **40**, 893 (1968)
5. Fujiwara, Y., Tamagaki, R.: A study on three-alpha structure of ^{12}C in the Faddeev formalism. Prog. Theor. Phys. **56**, 1503 (1976)
6. Kamada, H., Oryu, S.: The three-alpha Faddeev calculation on ^{12}C bound states with the Pauli corrected alpha–alpha potential. Prog. Theor. Phys. **76**, 1260 (1986)
7. Kircher, R., Kamada, H., Oryu, S.: A comparison of the off-shell α–α and α-N scattering amplitudes of different separable potentials. Prog. Theor. Phys. **73**, 1442 (1985)
8. Smith, E., Woodhouse, R., Papp, Z.: Refinement of the $n-\alpha$ and $p-\alpha$ fish-bone potential. Phys. Rev. C **86**, 067001 (2012)
9. Kamada, H., Koike, Y., Glöckle, W.: Complex energy method for scattering processes. Prog. Theor. Phys. **109**, 869 (2003)
10. Esbensen, H., Bertsch, G.F., Hencken, K.: Application of contact interactions to Borromean halos. Phys. Rev. C **56**, 3054 (1997)
11. Afnan, I.R., Thomas, A.W.: Modern Three-Hadron Physics. pp. 1 Springer, Berlin (1977)

12. Oryu, S., Kamada, H., Sekine, H., Yamashita, H., Nakazawa, M.: Calculation of ${}^{9}_{\Lambda}$Be in an $\alpha - \alpha - \Lambda$ three-body model using the Faddeev equations. Few-Body Sys. **28**, 103 (2000)
13. Kukulin, V.I., Krasnopol'sky, V.M., Voronchev, V.T., Sazonov, P.B.: Detail study of the cluster structure of light nuclei in a three-body model. Nucl. Phys. A **453**, 365 (1986)
14. Zhukov, M.V., Danilin, B.V., Fedorov, D.V., Bang, J.M., Thompson, I.J., Vaagen, J.S.: Bound state property of Borromean halo nuclei: ^{6}He and ^{11}Li. Phys. Rep. **231**, 151 (1993)
15. Suzuki, Y.: The ground-state structure and the Soft Dipole mode of the ^{6}He nucleus. Nucl. Phys. **A528**, 395 (1991)
16. Tilley, D.R. et al.: Energy Levels of light nuclei A = 6. Nucl. Phys. **A708**, 3 (2002)
17. Pieper, S.C., Wiringa, R.B.: Quantum Monte Carlo calculations of excited states in A = 6–8 nuclei. Phys. Rev. C **70**, 054325 (2004)
18. Kamada, H., Yamaguchi, M., Uzu, E.: Core-excitation three-cluster model description of ^{8}He and ^{10}He. Phys. Rev. C **88**, 014005 (2013)
19. Uzu, E., Kamada, H., Koike, Y.: Complex energy method in four-body Faddeev–Yakubovsky equations. Phys. Rev. C **68**, 061001(R) (2003)
20. Deltuva, A., Fonseca, A.C.: Neutron-^{3}H scattering above the four-nucleon breakup threshold. Phys. Rev. C **86**, 011001(R) (2012)
21. Phyu, A.M., Kamada, H., Golak, J., Oo, H.H., Witała, H., Glöckle, W.: The complex energy method applied to the Nd scattering with a model three-body force. Prog. Theor. Phys. **127**, 1033 (2012)